

Feasibility of amide proton transfer imaging of rodent glioblastoma model at 3T clinical scanner

Jinsuh Kim¹ and Phillip Zhe Sun²

¹Radiology, University of Iowa, Iowa City, IA, United States, ²Radiology, A. A. Martinos Center for Biomedical Imaging, Massachusetts General Hospital, Boston, MA, United States

Introduction:

Chemical exchange saturation transfer imaging (CEST), specifically amide proton transfer (APT) imaging, has demonstrated a promising potential in biomarker of brain tumor activity which may become a valuable tool in evaluating therapeutic response to glioblastoma (GBM)¹. Despite preclinical imaging on GBM xenograft models is crucial to test validity and reliability of this new technique, CEST/APT imaging on small animals generally requires ultrahigh field strength micro-MRI facilities which are not widely available to many researchers. Lack of easy access to small animal MRI facility and demand for high fidelity data acquisition have been hampering clinical translation of APT imaging. Variable density (VD) spiral sequence has many desirable properties that come from its concentric circular geometry allowing oversampling near the origin of *k*-space and reduced hardware demand on gradient switching; hence efficient use of gradient power². In this work, we developed a new CEST/APT imaging sequence with *k*-space trajectory of 2D interleaved VD spiral-out. We applied this method on orthotropic GBM xenograft models in immune-deficient rats to test feasibility of preclinical APT imaging at clinical 3T scanner.

Methods:

Four male athymic nude rats (Hsd:RH-Foxn1^{mu}) 7-8 weeks of age were implanted with U87 MG cells in the right frontal caudate region stereotactically, and imaged at 20-25 days after tumor implantation on a 3T clinical MRI scanner equipped with a quadrature transmit/receive RF coil (I.D. of 38 mm). Local shimming was followed by acquisition of multi-shot VD spiral-out APT-weighted images with 31 pulsed saturation RF irradiation ($B_1=1.5 \mu\text{T}$) and 21 frequency-labeling offsets from -5 ppm to 5 ppm with respect to water (TR/TE=1600/1.7 msec, spiral interleaves=20, slice thickness=3 mm, FoV=40 mm, matrix=96x96, average=2, acquisition time=14:25 min). B_0 inhomogeneity was corrected with Z-spectrum fitting on double-echo gradient field maps. The APT effect was calculated based on the MT-ratio asymmetry: $\text{MTR}_{\text{asym}}(3.5\text{ppm}) = 100\% \times [I_{\text{sat}}(-3.5\text{ppm}) - (I_{\text{sat}}(3.5\text{ppm}) / I_0)]$ ³. Additionally T1 mapping with variable flip angle FLASH, T2 mapping with multi-echo turbo SE, and ADC mapping on RESOLVE DWI with a three-point multi-exponential fitting ($b=0$, 1000 and 2800 s/mm^2) were performed.

Results:

Figure 1 shows the Z-spectra and APTR plots from each GBM xenograft model. APT ratio measured from the tumors were ranged from 3.40 to 5.28% (4.2 ± 0.83 ; mean \pm S.D.) higher than those from the normal side of the brain (Table 1). Figure 2 shows an example images of T1 map (A), T2 map (B), ADC map (C), APTR map (D), and histopathologic correlation of a U87 GBM xenograft (E,F).

Discussion:

Efficient use of gradient hardware in VD spiral sequence allowed small field-of-view acquisition while maintaining reasonable signal-to-noise ratio for small animal brain scan at clinical 3T scanner. This method can also significantly reduce scanning time and still maintain spatial resolution which are desirable attributes for practical translation of APT-weighted imaging. Enhanced APT effect within the GBM compared to the normal brain were consistent with previous report⁴. In this small study, we observed a trend of APT effect measures positively correlate with degree of pseudopalisading necrosis within the GBM on microscopy, which needs to be further investigated in a larger scale study.

References:

[1] Zhou J. et al., *Nature Med.*, 2011;17:130-4. [2] Kim D. et al., *Magn. Reson. Med.*, 2003;50:214-19. [3] Zhou J., *Methods. Mol. Biol.*, 2011;711:227-37. [4] Zhou J. et al., *Magn. Reson. Med.*, 2003;50:1120-26.

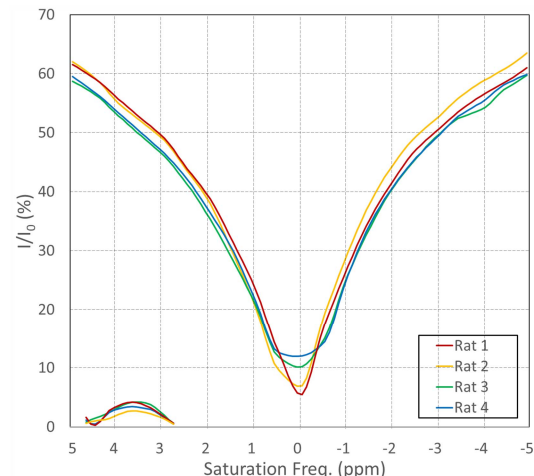


Figure 1

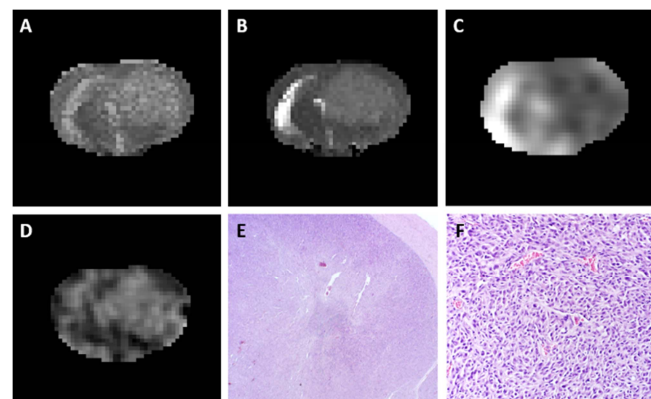


Figure 2

Table 1

GBM bearing rats	APTR (%)	T1 (ms)	T2 (ms)	ADC ($\times 10^3 \text{ mm}^2/\text{s}$)
1	5.28	1479.1	157.41	0.60
2	3.71	1545.2	172.89	0.46
3	4.38	1407.4	151.06	0.54
4	3.40	1262.9	196.12	0.51